ADVANCED ENGINEERING MATERIALS

DOI: 10.1002/adem.201000104

Functional Adhesive Surfaces with "Gecko" Effect: The Concept of Contact Splitting**

By *Marleen Kamperman, Elmar Kroner, Aránzazu del Campo, Robert M. McMeeking* and *Eduard Arzt**

Nature has developed reversibly adhesive surfaces whose stickiness has attracted much research attention over the last decade. The central lesson from nature is that ''patterned'' or ''fibrillar'' surfaces can produce higher adhesion forces to flat and rough substrates than smooth surfaces. This paper critically examines the principles behind fibrillar adhesion from a contact mechanics perspective, where much progress has been made in recent years. The benefits derived from ''contact splitting'' into fibrils are separated into extrinsic/intrinsic contributions from fibril deformation, adaptability to rough surfaces, size effects due to surface-to-volume ratio, uniformity of stress distribution, and defect-controlled adhesion. Another section covers essential considerations for reliable and reproducible adhesion testing, where better standardization is still required. It is argued that, in view of the large number of parameters, a thorough understanding of adhesion effects is required to enable the fabrication of reliable adhesive surfaces based on biological examples.

[*] *Prof. E. Arzt, Dr. M. Kamperman, E. Kroner*
INM – Leibniz Institute for New Materials, Functional Surfaces Group, and Saarland University
Campus D2 2, 66123 Saarbruecken, Germany
E-mail: eduard.arzt@inm-gmbh.de
Dr. A. del Campo
Max-Planck-Institut für Polymerforschung
Ackermannweg 10, 55128 Mainz, Germany
Prof. R. M. McMeeking
INM – Leibniz Institute for New Materials, Modeling/Simulation Group and Department of Mechanical Engineering, University of California Santa Barbara, CA 93106, USA

[**] *We acknowledge the contribution of numerous students, coworkers, and colleagues at the INM – Leibniz Institute for New Materials, Saarbrücken: Emerson De Souza, Roya Maboudian, Joachim Blau, Dadhichi Paretkar, Graciela Castellanos, and Jessica Kaiser. This work was funded by the Volkswagen Stiftung and by Deutsche Forschungsgemeinschaft (DFG) in conjunction with the EC Sixth Framework Programme, under contract N.ERAS-CT-2003-980409, as part of the European Science Foundation EUROCORES Programme FANAS.*

1. Introduction

The design of new functional surfaces often follows unexpected paths: e.g., windows are easier to clean when their surfaces are not perfectly smooth, but have a particular roughness; swimmers clad in special suits have broken world records because of the lower resistance offered by the water (these suits have recently been banned from international competition); lenses with roughened surfaces reflect less light and produce better pictures; and, maybe soon, reusable adhesives will be made more sticky by creating three-dimensional surface patterns.

In all of these cases, it is a particular micro- or nanopattern—often in the form of microfibrils—that creates a significant benefit over perfectly flat surfaces. The associated mechanisms, being largely counter-intuitive, were not invented by man but appeared in the course of evolution (Fig. 1): the lotus leaf and other plants have self-cleaning properties, maximizing the energy production through photosynthesis;[1] sharks move more efficiently in water because the ripples on their skin mute the effects of turbulence;[2] the eyes of moths and other insects have

Marleen Kamperman *received an M.Sc. degree in Chemistry in 2003 from the University of Groningen, The Netherlands. She continued her studies at Cornell University, Ithaca, NY, where she joined the group of Prof. Ulrich Wiesner in the Materials Science and Engineering department and worked on the development of ordered mesoporous high temperature ceramics using block copolymers. After finishing her Ph.D., in 2008, she joined the Functional Surfaces group of Prof. Eduard Arzt at INM – Leibniz Institute for New Materials in Saarbrücken, Germany, as a postdoctoral researcher, where she works on the development of bioinspired actuated adhesive systems.*

Elmar Kroner *studied materials science at the University of Stuttgart and the Max Planck Institute for Metals Research in Stuttgart, Germany. After a scholarship for a research stay at the University of California/Santa Barbara, he wrote his diploma thesis on contraction behavior of heart muscle cells on microstructured polymer surfaces. Currently, he works on bioinspired adhesive surfaces for a doctorate at the INM – Leibniz-Institute for New Materials in Saarbrücken.*

Aránzazu del Campo *received her Ph.D. in Chemistry from the Instituto de Ciencia y Tecnología de Polímeros in Madrid, Spain in 2000. She then joined the Max Planck Institute for Polymer Research in Mainz, Germany, as Marie Curie Fellow and started to work in the field of surface chemistry and nanotechnology. After a short stay at the Universitá degli Studi di Urbino, Italy, she moved in 2004 to the Max Planck Institute for Metals Research in Stuttgart and in 2007 to INM – Leibniz Institute for New Materials in Saarbrücken as group leader to work in the field of bioinspired adhesives. Since February 2009 she is a Minerva Fellow at the Max Planck Institute for Polymer Research in Mainz, heading the independent research group ''Active Surfaces and Materials.''*

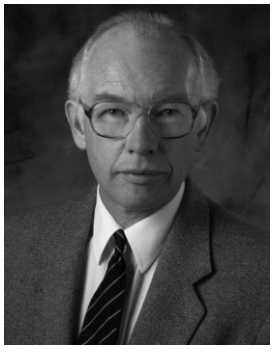

Robert M. McMeeking *earned a B.Sc. in mechanical engineering at the University of Glasgow, Scotland, and a Ph.D. in solid mechanics at Brown University. He was at Stanford University for 2 years working on metal forming problems. After 7 years at the University of Illinois at Urbana Champaign on the faculty of the Theoretical and Applied Mechanics Department, Dr. McMeeking moved to the University of California, Santa Barbara (UCSB) in 1985 as Professor of Materials and of Mechanical and Environmental Engineering. He was Chair of the Department of Mechanical and Environmental Engineering at UCSB in 1992–1995 and again during 1999–2003. In addition to his appointment at UCSB, Dr. McMeeking is Sixth Century Professor of Engineering Materials (Part-time) at the University of Aberdeen, Scotland, Visiting Professor of Materials Engineering at Saarland University, Germany, and External Member of the Leibniz Institute for New Materials, Saarbrücken.*

Eduard Arzt *is Scientific Director and Chairman at INM – Leibniz Institute for New Materials in Saarbrücken and holds the Chair for New Materials at Saarland University. He obtained his Ph.D. in Physics and Mathematics from the University of Vienna, Austria, in 1980. After a postdoctoral stay at the University of Cambridge, he led a research group at the Max Planck Institute for Metals Research in Stuttgart. From 1990 to 2007, he was a director at the Max Planck Institute for Metals Research, Stuttgart, and Professor for Metal Physics at the University of Stuttgart. He has been Visiting Professor at Stanford University and Massachusetts Institute of Technology and maintains strong links to the international materials community. His group in Stuttgart was among the first to tackle the problem of artificial gecko surfaces.*

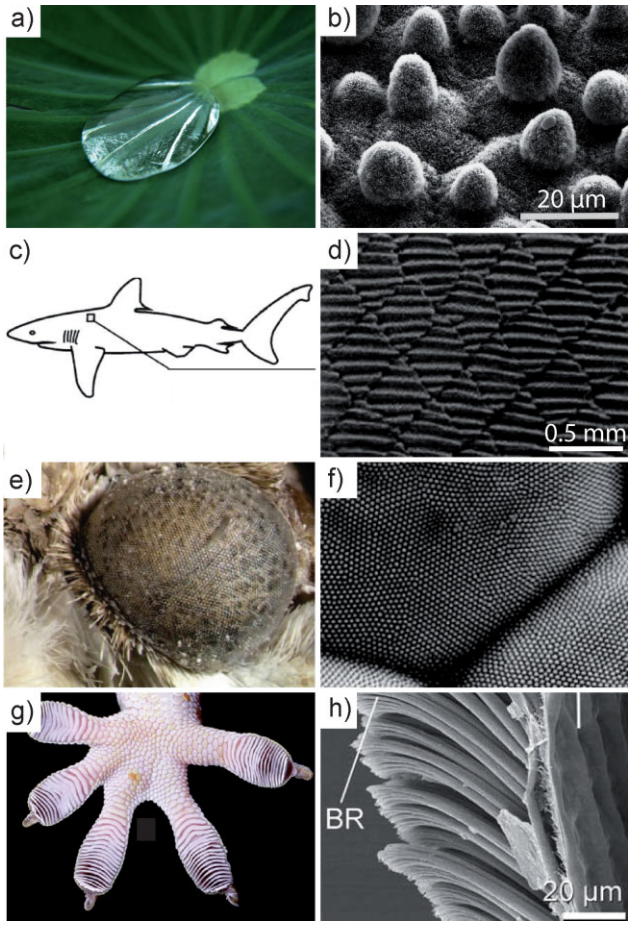

Fig. 1. Patterned surfaces in nature: (a) photograph and (b) scanning electron microscopy (SEM) image of lotus leaf.[1] (c) Cartoon and (d) SEM image of the scale structure of shark skin.[2] (e) Photograph and (f) SEM image of an antireflective moth's eye.[3] (g) Photograph and (h) SEM image of Gekko gecko adhesive structures. BR: branch.[45,127] Reproduced with permissions from Springer Link (a,b), E. Schweizerbart'sche Verlagsbuchhandlung, Science Publishers (c,d), Taylor & Francis and Mayo Foundation for Medical Education and Research (e,f), Company of Biologists and Elsevier (g,h).

anti-reflective properties;[3] and several animals, e.g., insects and geckos, owe their superior climbing and clinging ability to adhesion organs with microscopic fibrils.[4]

This paper focuses on artificial adhesive surfaces inspired by nature's example. Several research groups have synthesized such fibrillar structures over the last decade (for examples see Fig. 2). Initial efforts focused on the development of simple vertical fibrils with diameters in the micron range.[5,6] The first systematic variation of fibril diameters and aspect ratio was conducted by Greiner *et al.*;[7] it was clearly shown that polydimethylsiloxane (PDMS) exhibited size-dependent adhesion and that only the finest fibrils (diameter of 5 μm) exceeded unstructured PDMS control samples in adhesion strength. To fabricate more complex structures, closer in design, and performance to biological systems, combinations of patterning techniques were used. For example, photolithography and an inking method were used to manufacture fibers with mushroom-like tips.[8–13] The most systematic study to date is by del Campo *et al.*;[9] comparison of several contact shapes, among them spherical, flat punch, mushroom-like, and spatular tips, clearly confirmed the superiority of the mushroom shape, in some cases even surpassing the gecko adhesion limit. Recently, also tilted fibrils were modified with mushroom tips placed at a controlled angle with respect to the fibril.[10] Adhesion studies performed on these systems showed high directional adhesion, with shear forces almost six times higher in the gripping direction than in the releasing direction. Other advanced 3D geometries have been obtained by combining photolithography and dry etching methods.[14–18]

Some of the relevant fabrication methods are schematically summarized in Figure 3; they can be classified into micro/nanofabrication with or without the use of a template (Fig. 3a and b) and may contain an inking or coating step to modify the fibrillar structures after molding (Fig. 3c). Fabrication has been the subject of earlier reviews, e.g., by the present authors.[19–22]

Fibrillar adhesion is the manifestation of a seemingly simple concept that has been named ''contact splitting'':[23] adhesion can increase substantially when a single contact is split into many finer ones. The ramifications of this concept are, however, quite complex. In order to fully exploit this effect in artificial structures, a thorough understanding of the relevant contact mechanics is required.

Excellent reviews that cover certain aspects of the topic have been published, e.g.[19,24–30] The field is at present developing extremely rapidly; no article, including the present one, can capture all aspects and do justice to all authors in this subject. The present paper complements earlier articles by focusing on the current understanding of the mechanics of fibrillar contacts and on new aspects of adhesion testing.

2. Mechanics of Fibrillar Adhesion—The Effects of Contact Splitting

Adhesion between fibrillar surfaces and smooth substrates can be stronger than between two smooth surfaces.[6,31,32] Furthermore, patterns with small dimensions are often observed to be superior to those with a coarser scale.[7,33,34] At first sight, fibrillar or patterned surfaces seem to be at a disadvantage because they create less adhesion area with a substrate than a monolithic, continuous contact. This assessment, however, assumes that the adhesion force is proportional to the contact area, which in view of more detailed contact mechanics considerations is untenable. Fibrillar elements interacting with a substrate by short-range molecular effects (such as van der Waals forces) can exhibit higher adhesion due to several mechanisms. Following a similar categorization by Majumder *et al.*,[24] contact splitting effects can be grouped as follows (Fig. 4):

(i) Extrinsic contribution to the work of adhesion: fibrillar surfaces are more resistant to peeling because the strain energy stored in a fibril just before pull-off is not available to drive detachment of the next fibril. Another way

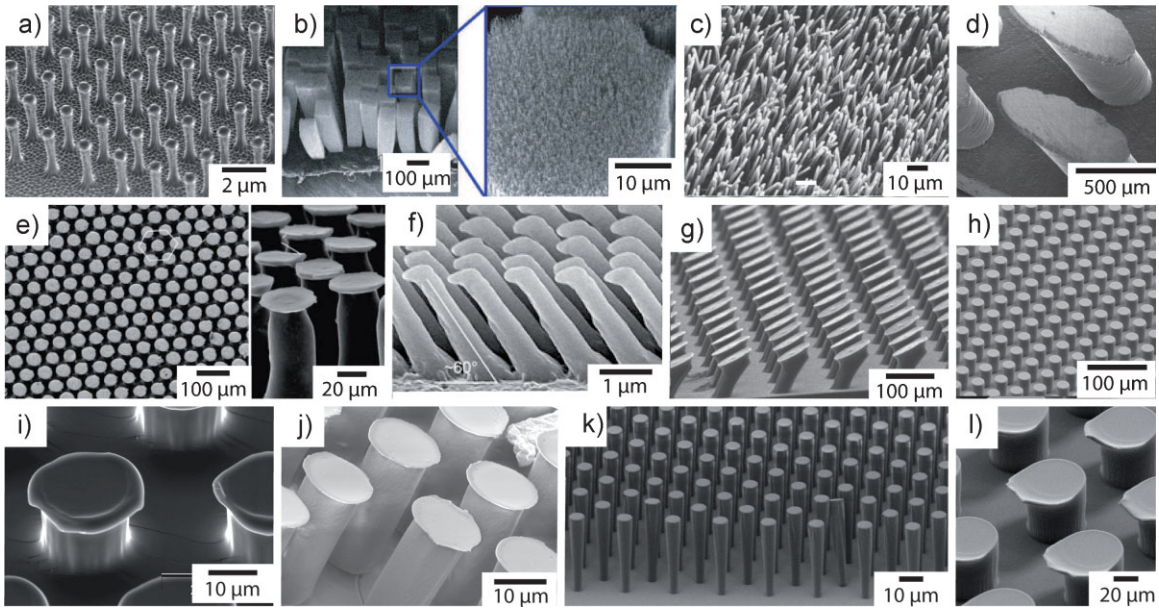

Fig. 2. Examples of fibrillar arrays fabricated by different methods (SEM micrographs). Direct nanofabrication without the use of a template by e-beam lithography (a)[5] or chemical vapor deposition (b).[85] Replication of templates by means of molding, using either porous membranes (c),[83] micromachined (d,e),[69,13] etched (f),[18] or photolithographic templates (h–l).[7,9,10] Reproduced with permissions from Nature Publishing Group (a), National Academy of Sciences (b), VSP (c,d), Royal Society Publishing (e), National Academy of Sciences (f), Wiley-VCH (g), and American Chemical Society (h, i, k, l).

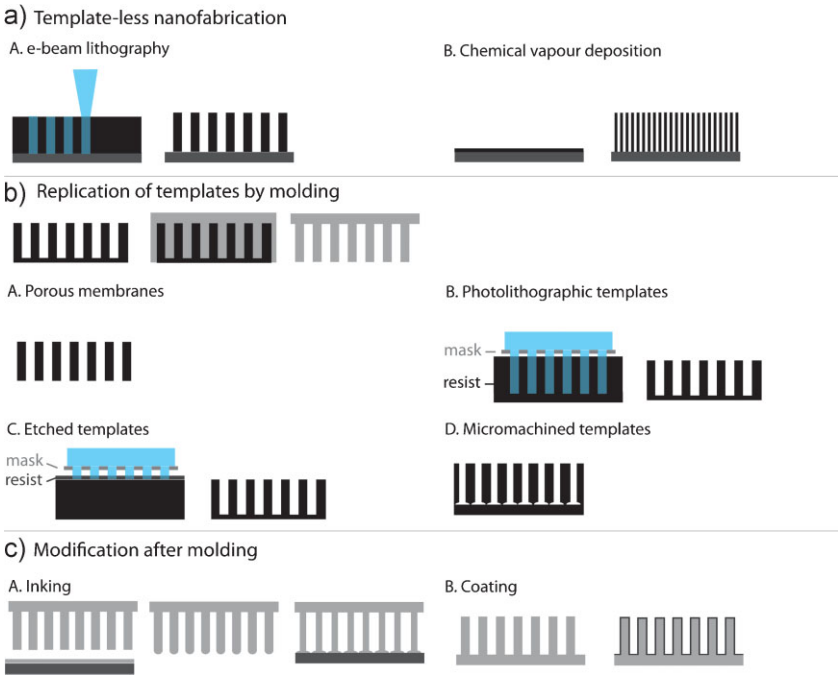

Fig. 3. Overview of fabrication methods used for fibrillar arrays. (a) Direct nanofabrication without the use of a template: (A) E-beam lithography was used to microfabricate polyimide pillars.[5] (B) Chemical vapor deposition was used to grow arrays of vertically aligned carbon nanotubes.[32,85–88,128] (b) Replication of templates by means of molding: (A) commercially available porous anodized alumina or polycarbonate membranes were used as mold directly.[6,66,82–84,129–133,134] (B) In photolithography, light is used to transfer a pattern from a mask to the resist on the substrate, resulting in molds with precise control over the geometric parameters.[7,9,17,33,63,64,92,104,135] (C) More complex molds were fabricated by a combination of photolithography and etching techniques.[14–18] (D) With micromachining, complex templates, but limited to relatively large feature sizes were fabricated.[62,69] (c) Modification of fibrillar arrays after molding by inking to produce different tip geometries (A),[8,9,10–12] or coating to modify the chemistry of the pillars (B).[71,124,136–139]

of putting it is that the detachment ''crack'' has to be re-initiated fibril by fibril, where re-nucleation of peeling is more difficult than its continuation.[35]

(ii) Adaptability to rough surfaces: long fibrillar elements can conform to roughness of the substrate with less strain energy penalty. This effect is most pronounced in hierarchical fibril systems.[36]

(iii) Size effect due to surface-to-volume ratio: for small contacts, the penalty associated with the distortion required for accommodation, being controlled by volume, vanishes more rapidly than the surface energy gain. This favors the adhesion of smaller contact elements.[23,37]

(iv) Uniform stress distribution: unlike larger contacts, adhesive contacts below a critical size have been shown to develop a uniform stress distribution at maximum adhesion strength before pull-off occurs. Bundles of very small adhering fibrils can thus collectively reach theoretical adhesion strength; in addition, they are more defect tolerant.[38]

(v) Defect control and adhesion redundancy: if adhesion defects control

ADVANCED ENGINEERING MATERIALS

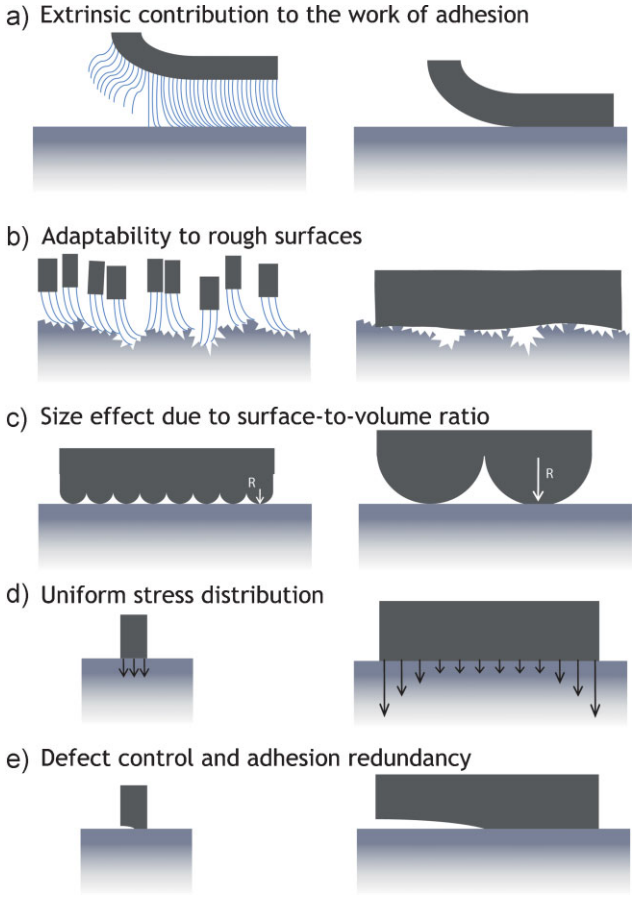

Fig. 4. Schematic representation of adhesion mechanisms in fibrillar surfaces identified to date (''contact splitting effects''): (a) extrinsic contribution to the work of adhesion; (b) adaptability to rough surfaces; (c) size effect due to surface-to-volume ratio; (d) uniform stress distribution; (e) defect control and adhesion redundancy. The overall effect on adhesion may be a superposition of some or all of these mechanisms.

detachment, it is better to have small defects; splitting up into finer contacts will limit defect sizes, and adhesion will be stronger. By contrast, a large defect in a monolithic contact is more damaging and will lead to easier detachment.[39]

A brief summary of adhesion basics will now be given, followed by a more detailed, critical discussion of the advantages of fibrillar systems.

2.1. Adhesion Basics Revisited

From the physical point of view, adhesion can be simplified to a traction law that defines the attraction between surfaces being brought adjacent to each other. If we consider two flat, parallel surfaces at a distance δ apart, the force per unit area of the attraction (the traction) is given by $T(\delta)$, where $\delta = 0$ is the configuration in which affinity between the surfaces is balanced exactly by quantum repulsion among the molecules. The work of adhesion, w, is then given by:[40]

$$w = \int_0^\infty T\mathrm{d}\delta \tag{1a}$$

The work of adhesion can also be written as:

$$w = \gamma_1 + \gamma_2 - \gamma_{12} \tag{1b}$$

where γ_1 and γ_2 are the surface energies of the materials when exposed to air or vacuum, and γ_{12} is the interface energy when the two surfaces are adhering to each other.[40] The interaction can be modeled in a variety of ways; a special case, often useful for obtaining insights on scales that are macroscopic compared to material interaction distances, is to take the distance over which the interaction is felt to be vanishingly small, but with w remaining finite; this implies that the attractive traction diverges. In this case, Equation (1a) loses its utility, but Equation (1b) still prevails. Other models of the interaction include the use of power law terms that provide the balance among attractive and repulsive forces; examples are a power law model of van der Waals interaction,[40] a Lennard–Jones model, and the Dugdale interaction, which assumes a traction T that is independent of δ up to a finite interaction distance δ_o and zero beyond there.[41] As a consequence, the work of adhesion is $w = T_o\delta_o$, where T_o is the attraction operating when $\delta \leq \delta_o$.

The complexity of adhesion arises when the two surfaces are no longer flat and hence accommodating deformations become important. The classic Johnson–Kendall–Roberts (JKR) concept[37] has received much renewed attention because of its applicability to biological structures. It invokes the elasticity of initially spherical surfaces, and combines this phenomenon with the work of adhesion for the case where the interaction distance is vanishingly small and the attractive forces are divergently large. The force required to form a circular contact of radius a is then given by:

$$P = \frac{4E^*a^3}{3R} - \sqrt{8\pi E^* a^3 w} \tag{2}$$

where E^* is the reduced elastic modulus:

$$\frac{1}{E^*} = \frac{1-\nu_1^2}{E_1} + \frac{1-\nu_2^2}{E_2} \tag{3}$$

with E_i being Young's modulus and ν_i Poisson's ratio, the subscript indicating a possible difference in material for each of the surfaces in contact. The reduced radius R is defined as:

$$\frac{1}{R} = \frac{1}{R_1} + \frac{1}{R_2} \tag{4}$$

where R_i are the radii of the two spherical surfaces in contact. Note that the model assumes infinitesimal strain of isotropic materials, and that a is much smaller than R_i. In load control, the magnitude of the tensile pull-off force turns out to be:

$$P_o = \frac{3}{2}\pi R w \tag{5}$$

In conditions that differ from load control, the pull-off force is less than given by Equation (5). For example, in displacement control, where the loading system is extremely stiff, the pull-off force magnitude is $5\pi Rw/6$, and for intermediate stiffness of the loading system, the pull-off force lies somewhere between this value and that given in Equation (5).

REVIEW

The pull-off force in Equation (5) is independent of the elastic properties, which is true only for the special case of spherical surfaces (see for example ref. [47] for different geometries). However, when the surfaces are very stiff, the radii of curvature of the surfaces are small, or the adhesion energy is high, the pull-off force in force control is given by a different equation due to Bradley[42] and Derjaguin *et al.* (referenced in[43]). If $R \gg \delta_o$, the pull-off force can be approximated as:

$$P_o = 2\pi R w \tag{6}$$

This result is known as Derjaguin, Muller, Toropov (DMT),[43] though strictly the DMT limit is subtly different.[41,44] Maugis suggested to parameterize conditions intermediate to the extremes of JKR and DMT by $T_o^3 R/w(E^*)^2$, with a value of zero representing the DMT case and ∞ the JKR one.[41] As has been pointed out by Gao *et al.*, the JKR, DMT, and Maugis results can all be manipulated to give a pull-off force that exceeds the peak strength of the adhesive attraction by selecting the Maugis parameter to be very small.[45] This unphysical situation arises because the surface area over which the attraction is being applied exceeds the available surface area, a situation that comes about because the asymptotic approximations utilized in the models are violated. Kim *et al.* commented on this point.[44] From a practical point of view, we note that Equation (5, 6) and the result for displacement control stated above all predict pull-off force values within about a factor of 2. This justifies the otherwise unqualified use of the JKR result in Equation (5) in several earlier publications.

Gao and Yao have pointed out that a small size can ensure that a protrusion remains adhered until the maximum adhesion strength of the surface interaction is exceeded.[38] The effect may be understood most clearly when the Dugdale law is used in conjunction with a hemisphere adhered to a rigid flat surface. When the radius of the hemisphere is very large, the pull-off force will be close to the JKR limit, rewritten as:

$$P_o = \frac{3}{2}\pi R_o \delta_o T_o \tag{7}$$

where R_o is the radius of this hemisphere that is large enough to be in the JKR limit. Now consider tiny hemispheres such that R is slightly larger than δ_o; these will not pull off at loads lower than the cross-sectional area of the hemisphere times the maximum adhesive strength, T_o. That is, the pull-off force for the very small hemispheres is at least:

$$P_o = \pi R^2 T_o \tag{8}$$

because all of its surface interacts adhesively with the rigid flat. We state Equation (8) as a lower bound, because the proximity of the surface from which the hemispheres protrudes may enhance the total force of interaction, especially if the material of the hemisphere is very compliant.

If we compare Equation (8) with (7), we find that the pull-off force for the small hemisphere is much smaller than that for the large one, simply because $R \ll R_o$. Now let the one large hemisphere be replaced by N small ones. By choosing $N = (R_o/R)^2$ we ensure that the nominal area of the adhering surfaces remains constant. It follows from Equation (8) that the pull-off load for the system of N small hemispheres becomes at least:

$$P_o = \pi R_o^2 T_o \tag{9}$$

If we now compare Equation (9) with (7), we see that the pull-off load for the array of many tiny hemispheres is much larger than that of the single large one, due to the fact that $R_o/\delta_o \ll 1$. In fact, we observe that since both the single large hemisphere and the array of tiny ones occupy a nominal area of adhering surface given by πR_o^2, the adhesive strength of the array of small hemispheres is T_o, whereas that of the single, large one is $3\delta_o T_o/2R_o$, and thus much smaller. On this basis, the array of very small hemispheres has an adhesion strength equal to the maximum adhesive interaction between the surfaces and is much more efficient than the single large one. Gao and Yao demonstrate that protrusions with shapes other than hemispherical can bring about similar benefits from this mechanism of adhesive strengthening.[38] While the maximum adhesive strength of the interaction between the surfaces is a strict limit on the quality of physical adhesion, getting close to it is advantageous. Practically, it seems desirable but difficult to texture surfaces with protrusions that are small enough to bring the adhesive strength close to the theoretical maximum.

2.2. Size Effects Due to the Trade-off between Strain and Adhesion Energy

It has been pointed out by Arzt *et al.*[23] that the pull-off force in Equation (5) scales with a geometrical length (not an area), giving rise to a size effect: imagine the replacement of one large spherical contact of radius R_o by N smaller ones of radius $R = R_o/\sqrt{N}$ with the same total (Hertzian) contact area (i.e., similar to the idea used above in which a single large contact is replaced by $N = (R_o/R)^2$ small ones); the pull-off force for simultaneous detachment of these N spheres will then be enhanced by a factor of $\sqrt{N}$:

$$P_o = \frac{3}{2}\pi\sqrt{N} R_o w \tag{10}$$

This concept is based on two assumptions that require further comment. The first is the validity of the JKR model even though the ratio a/R grows rapidly as the spheres become smaller. An estimate shows that for the elastomer PDMS with structure radii of $\sim$100 μm large strain effects occur which render the JKR approach questionable. Gao *et al.* have instead shown that the pull-off load lies below the JKR result for small spheres and approaches an asymptote in which the pull-off force is the peak strength of the adhesive interaction multiplied by the cross-sectional area of the hemisphere.[38,45] Therefore, we conclude that Equation (10) overpredicts somewhat the benefits of contact splitting when

the hemispherical radii become small. In any case, the maximum pull-off strength cannot exceed the peak strength of the adhesive interaction times the exposed surface area, giving a hard limit to the benefit of contact splitting, as discussed above.

The other critical assumption is that all spherical elements detach simultaneously. Instead it is possible that the elements will peel, i.e., begin to detach at one side of the large array. We now ask how such a mechanism would affect the pull-off force. As rice has pointed out in the context of a crack propagating through a compliant material bonded to two stiff platens that are subject to displacement control, steady propagation will occur when the strain energy released per unit surface area created is equal to the energy absorbed by the creation of the surfaces.[46] In the case of JKR behavior under tension, this will occur when the load applied to each hemisphere is $4\pi Rw/3$. It follows that detachment by steady state peeling of a fibrillar surface consisting of N hemispheres of radius $R_o/\sqrt{N}$, backed by stiff platens, will occur when:

$$P_d = \frac{4}{3}\pi\sqrt{N}R_o w \tag{11}$$

Comparison of Equation (10) and (11) shows that peeling under the specified conditions degrades the pull-off force only slightly, and the benefit of contact splitting is retained.

2.3. The Effect of Fibril Shape

The end of the fibril may be given other shapes besides hemispherical ones.[9] The contact splitting effect has been analyzed theoretically for a number of shapes by Spolenak *et al*.[47] When a *stiff* fibril with a punch-shaped flat end is attached to the flat surface of a *compliant* material, the analysis of Kendall may be utilized, at least when there is negligible friction at the interface, and the degree of adhesion is modest.[48] The pull-off load is then:

$$P_o = \sqrt{8\pi E^* w R^3} \tag{12}$$

From this, it can be deduced that the pull-off force for such a punch scales in proportion to $N^{1/4}$ for N smaller fibrils with the same area of the fibrillar surface; the contact splitting power is less than in the case of spherical shapes. Considerations similar to those discussed above for hemispheres suggest that there is little penalty as far as the pull-off force is concerned when peeling occurs through the forest of fibrils, rather than simultaneous detachment. Note also that the pull-off force is limited to the peak strength of the adhesive interaction multiplied by the cross-sectional area of the fibril, so that there must be an asymptotic transition to this result from that given in Equation (12) when the right hand side increases toward that limit.

It is emphasized that the analysis of Kendall only applies to a very stiff fibril adhered to a compliant material, but not to a compliant, flat ended fibril adhering to the flat surface of a very stiff material.[48] Gao *et al*. have provided a correct, if specialized analysis by assuming a detached annulus around the perimeter of the adhesion.[45] The pull-off force for one fibril is then:

$$P_o = \left(\frac{a}{R}\right)^{\frac{3}{2}} S\sqrt{8\pi E^* w R^3} \tag{13}$$

where S is a shape function dependent on a/R. Therefore, the adhesion strength in this case depends on the depth of the perimeter detachment. A useful result is that S varies little for $0 \le a/R \le 0.8$, falling from 1.25 to 1 in that range. For $a/R = 0.8$ $(a/R)^{3/2}$ is 0.7.[45] However, as a/R approaches unity, S goes to ∞, since the driving force for detachment is provided by the severe stress intensification at the edge of the detachment. The result of the model represented by Equation (13) is invalid in that limit, though a finite radius of curvature at the edge of the fibril tip can play the role of an annulus of detachment.[49] The Gao *et al*. analysis has the limitation that a detachment depth must be chosen to enable a definite result; the detachment depth may be calibrated by experiment, but otherwise it can only be chosen in an approximate way to ensure reasonable results.[45]

2.4. Defect-Controlled Detachment

The idea that detachment defects can control adhesion failure has previously been proposed by Hui *et al*., but has not received much attention in the field.[31] In previous investigations,[10,13,18,50] it was found that a fibril having a flanged end (i.e., the shape of the fibril resembles a mushroom) has a higher pull-off force, when separated from nearly flat surfaces of sapphire, than one having a simple punch shape, where the comparison is made for fibrils having the same shaft diameter. Spuskanyuk *et al*. have proposed an explanation for the behavior that is based on the presence of defects in the form of small detached regions around the perimeter.[51] Once peeling begins from the detachment defect, it will continue in an unstable manner under load control, since the stress on the remaining ligament will be steadily increased as the peeled area in the defect zone expands. In the case of the mushroom shaped fibrils, the stress at the perimeter of the flange is low in both the friction-free case and when there is friction.[51] As a consequence, it takes a much higher applied load to initiate a peel separation of the adhesion.

Quantification of the model requires a determination of the size, shape, and location of the defects, and thus experiments are required for this aspect, either by microscopic inspection of the detachment or pull-off tests with single fibrils. In this regard, the model suffers from the same challenges as the Gao *et al*. analysis of adhesion for the compliant punch against a flat, stiff surface.[45] However, if the defect characteristics are the same for both types of fibrils, a comparison can be made by quantifying the stress in the adhesion in the absence of detachment defects.[51] The predictions for the ratio of pull-off forces for the two types of fibrils are in reasonable accord with the data, with the important feature that the model involves a pull-off force for the mushroom that is several times greater than that of the punch.

McMeeking *et al*.[39] used the idea of defect control to model successfully the pull-off force for arrays of identical punches composed of PDMS, backed by a flat PDMS foundation, when

they are adhered to flat surfaces of sapphire.[52] In the experiments it was found that the pull-off force for the array was proportional to the total length of the adhesion perimeter; i.e., the circumference of one fibril multiplied by the number of fibrils. No other valid correlation of the data with fibril parameters was found. It was postulated that defects are to be found only at the perimeter of the punch and assumed that the size of the detachments obeyed a Weibull probability distribution function.[39] A correlation of the pull-off force with $N\pi R^2$ (the total *area* of adhesion) was shown to arise from a probability distribution heavily clustered around a single size of detachment defect (i.e., essentially deterministic), whereas the correlation of the pull-off force with $2N\pi R$ (the total *length* of the perimeter of the adhesion) was consistent with a very wide distribution of detachment defect sizes. As a consequence, it was deduced that the fibrils had such a wide distribution of detachment defect sizes at the perimeter of the adhesion. It should be noted that Varenberg *et al*.[52] found that the pull-off force of arrays of dimples also correlated with the total length of perimeter, a result that remains so far unexplained.

2.5. Strain Energy: Driving Force versus Extrinsic Toughness Contribution

In many cases in nature, the structure used for adhesion involves many long, slender fibrils. One advantage of these structures is, obviously, that they provide flexibility to allow conformation to surfaces of arbitrary roughness,[53] a virtue that is achieved both through fibril slenderness and via the common natural feature of a hierarchy of structure, especially in terms of size scale.[45] It is considered important that this conformity can be achieved in conjunction with low elastic strain energy, as this energy is usually a driver of detachment, an aspect that has been identified by Persson.[54] The slenderness of the structure, and its bending dominated deformation, allows surface conformity to occur with low strain energy, despite the fact that the natural materials utilized, such as β-keratin, are relatively stiff compared to synthetics such as PDMS.[36]

On the other hand, it has been proposed that long slender fibrils can enhance the toughness of adhesive systems by dissipation of stored elastic energy.[31,36,53,55] The reasoning behind this hypothesis is that the strain energy stored in a stretched fibril is lost when adhesive failure occurs, constituting an extrinsic contribution to the total work of adhesion. In a long fiber, the elastic strain energy just before pull-off is greater than in a short one with the same diameter; if we consider the fibril's strain energy to be lost upon detachment, much more dissipation of energy will occur for long fibrils. It is of some interest to determine whether such an extrinsic contribution to adhesion from this source is important. Extrinsic contributions to toughness are common in brittle materials, and without them many ceramics would be uselessly fragile.[56] In this regard, adhesion detachment and brittle fracture propagation are similar.[57] The common view in fracture mechanics is that the magnitude of the intrinsic contribution to fracture (the surface energy of the newly created surfaces of the crack) is negligible, but it gates the extrinsic processes that dissipate almost all of the fracture work. In fracture, such intrinsic mechanisms are associated with specific dissipaters of energy, such as plasticity, the motion of phase boundaries and friction. Without such a specific mechanism identified, it will remain unclear whether the strain energy stored in long fibrils is absorbed in an extrinsic contribution to adhesion and is thus beneficial. This unresolved issue can only be addressed by further research.

In summary, the concept of contact splitting, inspired by biological systems, has many potentially contributing mechanisms: extrinsic toughening, effect of surface-to-volume ratio, uniformity of stress distribution, and defect control. These mechanisms can superimpose to impart, even for totally smooth counter-surfaces, superior adhesion properties to fibrillar surfaces. In all cases, division into smaller contact elements and high aspect ratios should enhance adhesion, up to a theoretical maximum. The challenge is to fabricate such fine, sub-micron structures that do not suffer from instabilities, e.g., due to condensation or collapse. The limits of how fine such structures can be are illustrated in adhesion design maps.[58,59]

3. Adhesion Testing

This section will address some of the issues that arise in adhesion testing and then summarize important results obtained so far for fibrillar adhesives. The properties of fibrillar arrays have been investigated using a variety of testing methods in different laboratories. No standard test procedure is currently available, which limits the comparability of results from different authors. Our recent experiments have shown that the test results can be very sensitive to the details of the test method. Conversely, reliable data produced on well-calibrated devices can produce much insight into the detachment mechanisms of fibrillar structures.

3.1. Force-Displacement Curves

As a test probe, frequently spherical probes have been used; this helps circumvent alignment problems but, at the same time, complicates the interpretation of the data. The probe is brought in contact with the sample, applying a defined compressive load (preload) perpendicular to the sample surface; it is then retracted while force and displacement are measured. Test methods can be classified by the direction of the force measured during the experiment with respect to the sample surface (Fig. 5). True ''adhesion'' tests require application of a tensile load normal to the sample surface (Fig. 5a).[5–7,9,11,14,21,31–33,60–78] In shear (or friction) experiments, the sample is moved tangentially to the sample surface (Fig. 5b).[79–91] During a peel-test, the sample is peeled off one end of the substrate at a defined angle (Fig. 5c).[78,85,92–95] Recent studies demonstrated that normal and shear forces are

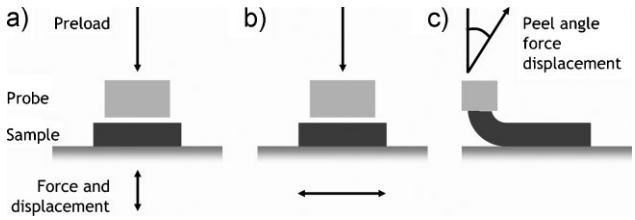

Fig. 5. Classification of adhesion tests. (a) Normal adhesion: force and deflection are measured parallel to normal preload. (b) Shear test: force and deflection are measured perpendicular to normal preload. (c) Peel test: sample is peeled from substrate under a defined angle.

coupled in an interesting way for fibrillar adhesives.[79–81,84,91,96,97] Modified setups have therefore been proposed to combine shear, normal, and/or peel modes.[10,79,83,91,98] Pull-off forces can be measured using weight balances,[66,86] load cells,[62,65,69] by cantilever deflection of AFMs or with AFM-like devices,[5–7,9,11,21,63,64,71–73,99] by surface-probe microscopes,[5,6,32,60,64,67,100] and with nanoindentation setups.[14,70,74]

A typical force-displacement curve for a normal pull-off experiment using a spherical probe is shown in Figure 6. After a specified compressive preload has been applied, the pull-off force is measured as the maximum of the tensile force applied. The work of adhesion is related to the area covered by the force-displacement curve.

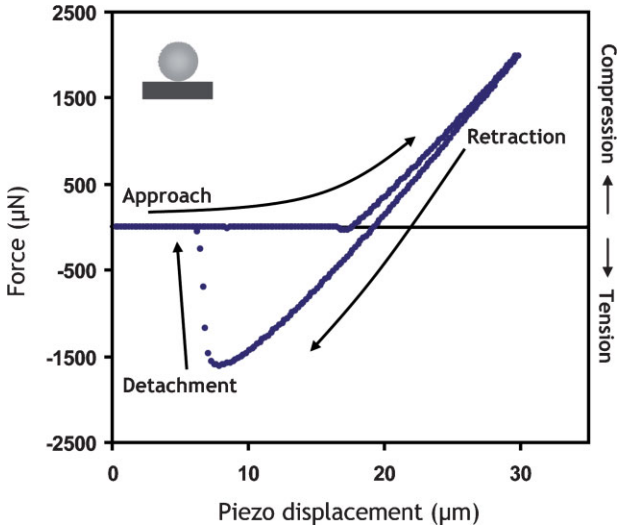

Fig. 6. Force displacement curve for a normal adhesion test with a spherical glass probe (4 mm diameter) on flat PDMS. Sample approaches the probe, contact is formed and the soft sample is compressed with a defined preload, and then retracted until detachment occurs at a certain pull-off force. The maximum of the tensile force is defined as the pull-off force. Note that in contact mechanics tensile forces are designated as negative, compressive forces as positive.

3.2. Effect of Probe Geometry

Force values obtained by different adhesion experiments are not directly comparable, as they depend on the contact area and thus on the geometry of the probe. For spherical probes it was shown that the pull-off force of fibrillar surfaces strongly increases with the applied compressive preload until it reaches a plateau (Fig. 7a).[7,33,50,75] Schargott *et al.*[101,102] and, more recently, Long and Hui[103] formulated models which describe the contact between an array of fibrils, simulated as independent elastic springs, and a spherical probe (Fig. 7b). Such models predict both a preload dependence of the pull-off force and a plateau value, which qualitatively fits experimental observations.[7,9] We note in passing that these models should, in the limit of infinitely fine springs, reduce to the JKR (Eq. 5) or DMT (Eq. 6) model; the preload dependence should then be lost for surfaces without fibrils.

Another complication of tests with spherical probes is that the contact area changes continuously during the measurement. In order to obtain contact *strength* values, the forces need to be normalized by the contact

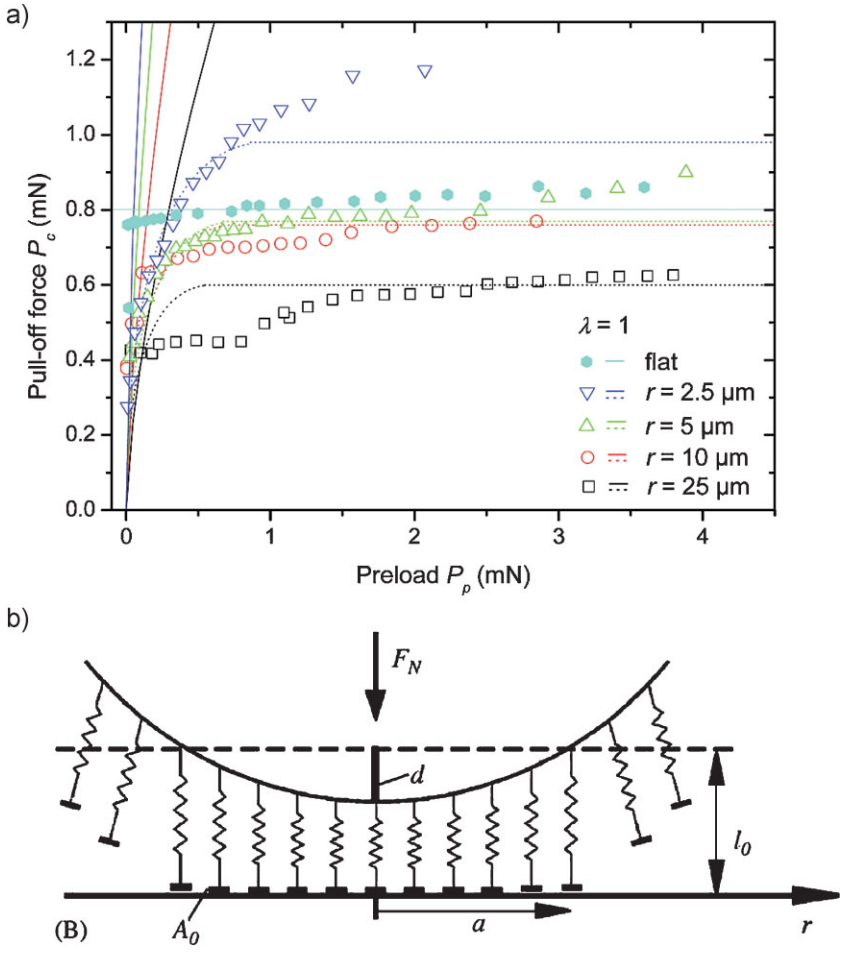

Fig. 7. Dependence of the pull-off force on the preload when a large sphere is used as probe: (a) experimental results on flat and fibrillar PDMS surfaces with fibrils of different radii.[7] The dotted lines represent the theoretical values according to the spring model, schematically depicted in (b).[101] Reproduced with permission from American Chemical Society and from Elsevier.

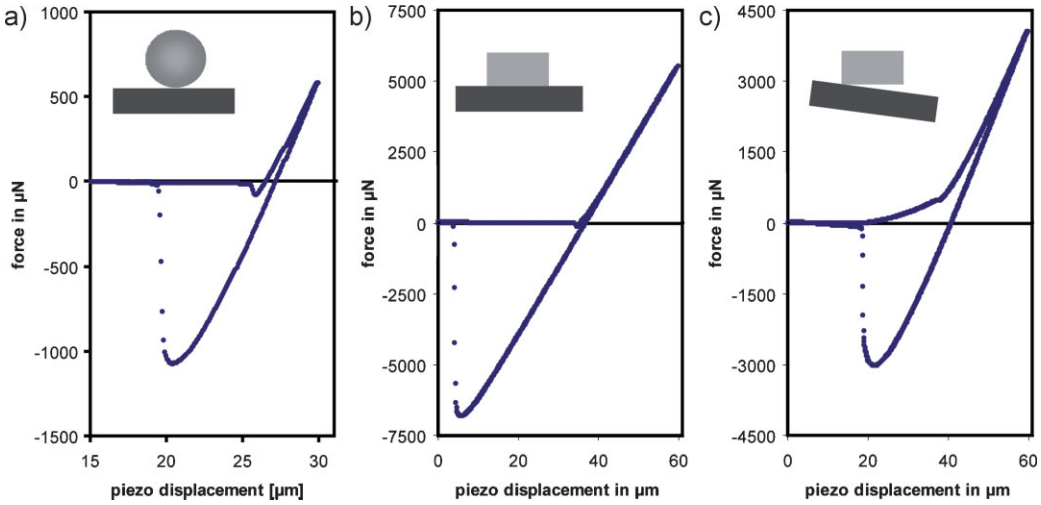

Fig. 8. Adhesion measurements with different probe geometries and misalignments: (a) spherical glass probe (4 mm diameter), (b) flat silicon probe (~0.5 mm^2) with good, and (c) with poor alignment on flat PDMS. Thevalue of the pull-off force is very sensitive to these changes. Note that the scaling of the abscissa is different on all three curves.

area.[32,67,68,104,105] This necessitates either the calculation of the contact area from the displacement data or, even better, in situ visualization using a microscope.[31,33,61,63,75–78] The change in contact area during the detachment phase is for structured surfaces even more complex, especially for relatively small probe diameters, as single fibrils or fibril clusters detach in a stepwise fashion, leading to non-circular contact areas.[33]

To overcome the problems of changing contact area and inhomogeneous strain fields within the sample, adhesion experiments with flat probes were recently performed and compared to tests with spherical probes.[106] The results did not show any dependence of the pull-off force on preload, as in earlier experiments.[13,52,89,107,108] The comparative study however highlighted the main draw-back of flat probes: normal pull-off experiments require extremely careful alignment of sample and probe. A (controlled) misalignment of only 2° resulted in a pull-off force reduction by about 50% for a flat PDMS sample (Fig. 8). Conversely, the misalignment of probe and sample can be conveniently determined by analyzing the resulting force displacement curves.[109]

3.3. Repeated Pull-off Measurements

Artificial fibrillar adhesives may be of special interest for repeated attachment-detachment cycles. Recently, Kroner *et al*. (see Kroner *et al*. in this issue) performed repeated adhesion measurements with the same PDMS sample and found significant changes in force-displacement curves. The pull-off force was found to drop characteristically during the first probe-sample contacts, followed by a leveling off after several hundreds of contacts. While the initial force values depended on various fabrication parameters, the plateau found after about 1000 contacts was independent of the fabrication protocol. These effects were explained by a transient transfer of free oligomers from the sample to the probe, changing the surface energy and thus the pull-off force. This effect was observed on both fibrillar and flat surfaces, but was much more pronounced for fibrillar arrays. Further experiments along these lines will be necessary to ascertain the mechanisms and to qualify certain polymers for repeated detachment applications.

3.4. Summary of Fibril Geometry-Adhesion Relationships

The large amount of adhesion data for fibrillar arrays collected over the last years allows some general trends to be identified:

(i) Size effect: the adhesion force and strength of fibrillar surfaces increase significantly with decreasing fibril radii.[7,33,34] The pull-off strength of fibril arrays with flat tips, increased with $r^{-0.4}$, where r is the fibril radius (at constant aspect ratio).[7] The exponent, termed ''splitting efficiency,'' quantifies the potential for improving the adhesion strength by decreasing the contact size.[47]

(ii) Aspect ratio effect: fibrils of varying lengths at constant fibril radius show an increase in adhesion force with increasing aspect ratio.[7] This is attributed to the higher elastic energy dissipated at pull-off, see also Section 2.5.[6,9,20,58] At least one other report claims that the aspect ratio did not have an effect on adhesion.[77] Peeling experiments have shown that, for low aspect ratio fibrils, most of the stored elastic energy dissipated upon detachment comes from the deformation of the backing layer, while for high aspect ratios, it comes from bending of the fibrils. The bending contribution increases with aspect ratio, leading to increased adhesion up to a limiting value due to buckling and condensation of fibrils.[92]

(iii) Shape effect: among different tip geometries, mushroom-shaped tips have so far given the highest adhesion strength values of all polymeric fibers.[9–11,21,110,111] They

also show the highest potential for adhesion enhancement by contact splitting.[9]

(iv) Hierarchy effect: theoretical studies have predicted a beneficial effect of hierarchy in adhesion.[112–116] However, two-level structures produced so far showed a drop in adhesion as compared to single-level structures.[117] Shear adhesion strength was also reduced for hierarchical structures.[18] To date, only hierarchical structures containing macroscopic first-level fibrils succeeded in increasing adhesion.[118]

(v) Effect of backing layer: the adhesion performance has been shown to increase with decreasing thickness of the backing layer.[65,119] This was explained by a more equal load sharing for thinner backing layers during pull-off resulting in higher adhesion. Thick backing layers deform during pulling and this leads to stress concentrations at the edge of the substrate, similar to a rigid punch in adhesive contact with a half space.[120] In a recent study, it was demonstrated that the fibrils ''communicate'' mechanically through the backing layer, giving interesting effects in discrete pull-off of individual fibrils.[121]

4. Outlook: Future of Gecko-Inspired Adhesives

The attachment organs of climbing animals like the gecko exhibit a unique combination of properties: strength, reversibility, reusability, directionality, durability, and a self-cleaning mechanism. Obviously, a fully functional gecko-inspired adhesive could find many potential applications, such as temporary fastening in the construction industry, temporary labeling, optimization of surfaces for sports equipment, biomedical materials and devices, and fixation for household items. For artificial surfaces to function as designed, the mechanical, structural, and chemical aspects have to be optimized at the same time. This explains why the space of design parameters is so huge and why biomimetic fabrication is not a simple task.

As elaborated above, contact splitting into finer contact elements results in stronger adhesion for several independent reasons (Fig. 4). This is observed in different natural species and corroborated by experimental data. Finer contact elements will also enhance the adaptability to rough surfaces. Reduction of structural features of dry adhesives, however, requires material systems that are strong, tough, and durable, since small structures are prone to lateral collapse and fracture. Therefore, more efforts are required to develop materials that accommodate these requirements. Other prerequisites for the successful development of useful products lie in so far unexplored properties: how do gecko surfaces behave under repeated contact formation and breakage? How do they respond to changes in temperature and humidity?[122] What is their long-term reliability in specific environments? And, most important, how can they be fabricated cost-effectively over large areas? Only if these and similar problems can be successfully overcome, will gecko-inspired adhesives realize their potential in applications.

In addition to these general challenges, each individual application will require a separate set of requirements. For example, potential applications in the biomedical field require biocompatible or biodegradable materials and adhesion against soft, living, and complex viscoelastic material systems. So far, most of the dry adhesion systems have been tested against flat and stiff probes. A first study examined the applicability of such surfaces to mucosa surfaces.[123] Another study evaluated the adhesion performance against porcine intestine tissue.[124] In this study the maximum adhesion force did not correspond to the highest fibril density, which is not compatible with the current understanding of the ''gecko effect.'' At INM – Leibniz Institute for New Materials, Saarbrücken, a recent study of gecko surface adhesion to mouse skin revealed sufficient adhesion for possible application as ear implants.[125] There are also ongoing efforts at INM to determine the importance of the synthetic fibril geometry, surface chemistry, and stiffness in relation to soft probes for optimum adhesion in combination with cell behavior studies (see Eder *et al*. of this issue).

A promising new development is the creation of actuated adhesion systems. While stimuli-responsive adhesion has been demonstrated for conventional adhesives, reversible actuation of dry adhesives, e.g., through changes in the fibril orientation, is still in an exploratory stage. Reddy *et al*.,[126] for the first time, applied patterning strategies to shape-memory polymers to create microstructured surfaces with actuated adhesion (Fig. 9). The array of fibrils was mechanically deformed above its shape-memory transition temperature,

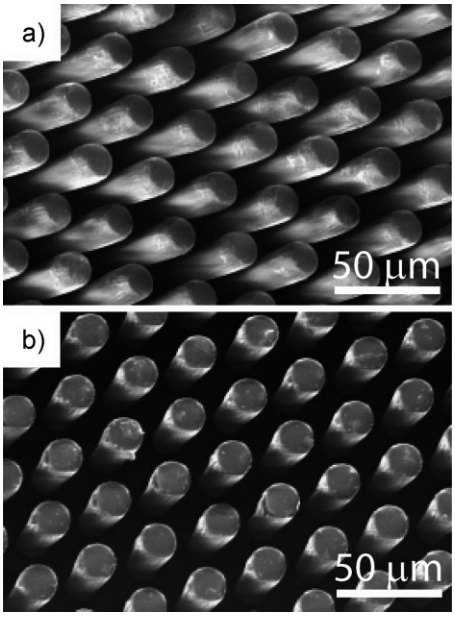

Fig. 9. SEM images of shape memory fibrils in the deformed tilted position (a) and of the recovered pillars after reheating (b).[126] This study demonstrates switching from a non-adhesive to an adhesive state. Reproduced with permission from American Chemical Society.

followed by cooling to room temperature in the deformed position. This yielded a temporary non-adhesive surface consisting of fibrils in a tilted position (Fig. 9a). By reheating above the transition temperature, the fibrillar surface switched back to a permanent adhesive state (Fig. 9b), with an adhesion force increased by a factor of 200. Magnetic fields were also used to activate a fully reversible adhesive comprising nickel cantilevers coated with vertically aligned polymeric nanorods.[105] These proof-of-principle studies demonstrate that van der Waals-based adhesion between two surfaces, one of which is fibrillar, gives the additional degree of freedom of switching adhesion on and off in a repeatable fashion. Now engineering development must take over to create useful material surfaces that may even surpass the gecko effect.

Received: March 3, 2010
Final Version: March 4, 2010
Published online: May 11, 2010

[1] W. Barthlott, C. Neinhuis, *Planta* **1997**, *202*, 1.
[2] W. E. Reif, *Courier Forschungsinstitut Senckenberg* **1985**, *78*, 1.
[3] J. Genzer, K. Efimenko, *Biofouling* **2006**, *22*, 339.
[4] K. Autumn, Y. A. Liang, S. T. Hsieh, W. Zesch, W. P. Chan, T. W. Kenny, R. Fearing, R. J. Full, *Nature* **2000**, *405*, 681.
[5] A. K. Geim, S. V. Dubonos, I. V. Grigorieva, K. S. Novoselov, A. A. Zhukov, S. Y. Shapoval, *Nat. Mater.* **2003**, *2*, 461.
[6] M. Sitti, R. S. Fearing, *J. Adhes. Sci. Technol.* **2003**, *17*, 1055.
[7] C. Greiner, A. del Campo, E. Arzt, *Langmuir* **2007**, *23*, 3495.
[8] A. Del Campo, C. Greiner, *J. Micromech. Microeng.* **2007**, *17*, R81.
[9] A. del Campo, C. Greiner, E. Arzt, *Langmuir* **2007**, *23*, 10235.
[10] M. P. Murphy, B. Aksak, M. Sitti, *Small* **2009**, *5*, 170.
[11] M. P. Murphy, B. Aksak, M. Sitti, *J. Adhes. Sci. Technol.* **2007**, *21*, 1281.
[12] M. Sitti, B. Cusick, B. Aksak, A. Nese, H.-I. Lee, H. Dong, T. Kowalewski, K. Matyjaszewski, *ACS Appl. Mater. Interfaces* **2009**, *1*, 2277.
[13] S. Gorb, M. Varenberg, A. Peressadko, J. Tuma, *J. R. Soc. Interface* **2007**, *4*, 271.
[14] M. T. Northen, K. L. Turner, *Nanotechnology* **2005**, *16*, 1159.
[15] M. T. Northen, C. Greiner, E. Arzt, K. L. Turner, *Solid-State Sensors, Actuators, and Microsystems Workshop*, Hilton Head Island, SC, U.S.A. **2006**, p. 43.
[16] D. S. Kim, S. H. Lee, C. H. Ahn, J. Y. Lee, T. H. Kwon, *Lab Chip* **2006**, *6*, 794.
[17] J. Davies, S. Haq, T. Hawke, J. P. Sargent, *Int. J. Adhes. Adhes.* **2009**, *29*, 380.
[18] H. E. Jeong, J. K. Lee, H. N. Kim, S. H. Moon, K. Y. Suh, *Proc. Natl. Acad. Sci. U. S. A.* **2009**, *106*, 5639.
[19] L. F. Boesel, C. Greiner, E. Arzt, A. Del Campo, to appear in *Adv. Mater.* **2010**.
[20] A. del Campo, E. Arzt, *Macromol. Biosci.* **2007**, *7*, 118.
[20] A. del Campo, E. Arzt, *Macromol. Biosci.* **2007**, *7*, 118.
[21] A. del Campo, C. Greiner, I. Álvarez, E. Arzt, *Adv. Mater.* **2007**, *19*, 1973.
[22] A. del Campo, E. Arzt, *Chem. Rev.* **2008**, *108*, 911.
[23] E. Arzt, S. Gorb, R. Spolenak, *Proc. Natl. Acad. Sci. U. S. A.* **2003**, *100*, 10603.
[24] A. Majumder, A. Sharma, A. Ghatak, *Bio-Inspired Adhesion and Adhesives: Controlling Adhesion by Micro-nano Structuring of Soft Surfaces in Microfluids and Microfabrication*, (Ed.: S. Chakraborty), Springer, USA **2010**, Ch. 7, pp. 283–307.
[25] H. E. Jeong, K. Y. Suh, *Nano Today* **2009**, *4*, 335.
[26] B. N. J. Persson, *J. Adhes. Sci. Technol.* **2007**, *21*, 1145.
[27] K. Autumn, N. Gravish, *Philos. Trans. R. Soc. A* **2008**, *366*, 1575.
[28] C. Creton, S. Gorb, *MRS Bull.* **2007**, *32*, 481.
[29] B. Bhushan, *Philos. Trans. R. Soc. A* **2009**, *367*, 1443.
[30] B. Bhushan, *Philos. Trans. R. Soc. A* **2009**, *367*, 1445.
[31] C. Y. Hui, N. J. Glassmaker, T. Tang, A. Jagota, *J. R. Soc. Interface* **2004**, *1*, 35.
[32] B. Yurdumakan, N. R. Raravikar, P. M. Ajayan, A. Dhinojwala, *Chem. Commun.* **2005**, 3799.
[33] A. J. Crosby, M. Hageman, A. Duncan, *Langmuir* **2005**, *21*, 11738.
[34] J. Y. Chung, M. K. Chaudhury, *J. Adhes.* **2005**, *81*, 1119.
[35] G. J. Lake, A. G. Thomas, *Proc. R. Soc. A* **1967**, *300*, 108.
[36] B. N. J. Persson, S. Gorb, *J. Chem. Phys.* **2003**, *119*, 11437.
[37] K. L. Johnson, K. Kendall, A. D. Roberts, *Proc. R. Soc. A* **1971**, *324*, 301.
[38] H. J. Gao, H. M. Yao, *Proc. Natl. Acad. Sci. U. S. A.* **2004**, *101*, 7851.
[39] R. M. McMeeking, E. Arzt, A. G. Evans, *J. Adhes.* **2008**, *84*, 675.
[40] J. N. Israelachvili, *Intermolecular and Surface Forces*, Academic Press, New York **1991**.
[41] D. Maugis, *J. Colloid Interface Sci.* **1992**, *150*, 243.
[42] R. S. Bradley, *Philos. Mag.* **1932**, *13*, 853.
[43] B. V. Derjaguin, V. M. Muller, Y. P. Toporov, *J. Colloid Interface Sci.* **1975**, *53*, 314.
[44] K. S. Kim, R. M. McMeeking, K. L. Johnson, *J. Mech. Phys. Solids* **1998**, *46*, 243.
[45] H. J. Gao, X. Wang, H. M. Yao, S. Gorb, E. Arzt, *Mech. Mater.* **2005**, *37*, 275.
[46] J. R. Rice, *J. Appl. Mech.* **1968**, *35*, 379.
[47] R. Spolenak, S. Gorb, H. J. Gao, E. Arzt, *Proc. R. Soc. A* **2005**, *461*, 305.
[48] K. Kendall, *J. Phys. D* **1971**, *4*, 1186.
[49] L. Ma, R. McMeeking, E. Arzt, *Int. J. Mater. Res.* **2007**, *98*, 1156.
[50] S. Kim, M. Sitti, *Appl. Phys. Lett.* **2006**, *89*, 261911.

[51] A. V. Spuskanyuk, R. M. McMeeking, V. S. Deshpande, E. Arzt, *Acta Biomater.* **2008**, *4*, 1669.
[52] M. Varenberg, A. Peressadko, S. Gorb, E. Arzt, *Appl. Phys. Lett.* **2006**, *89*, 121905.
[53] A. Jagota, S. J. Bennison, *Integr. Comp. Biol.* **2002**, *42*, 1140.
[54] B. N. J. Persson, *J. Chem. Phys.* **2003**, *118*, 7614.
[55] W. Federle, *J. Exp. Biol.* **2006**, 209. 2611.
[56] M. E. Launey, R. O. Ritchie, *Adv. Mater.* **2009**, *21*, 2103.
[57] A. A. Griffith, *Philos. Trans. R. Soc. Lond.* **1920**, *221*, 163.
[58] R. Spolenak, S. Gorb, E. Arzt, *Acta Biomater.* **2005**, *1*, 5.
[59] C. Greiner, R. Spolenak, E. Arzt, *Acta Biomater.* **2009**, *5*, 597.
[60] H. Lu, J. Goldman, F. Ding, Y. Sun, M. X. Pulikkathara, V. N. Khabashesku, B. I. Yakobson, J. Lou, *Carbon* **2008**, *46*, 1294.
[61] N. J. Glassmaker, A. Jagota, C. Y. Hui, J. Kim, *J. R. Soc. Interface* **2004**, *1*, 23.
[62] A. Peressadko, S. N. Gorb, *J. Adhes.* **2004**, *80*, 247.
[63] B. Aksak, M. P. Murphy, M. Sitti, *Langmuir* **2007**, *23*, 3322.
[64] E. S. Yoon, R. A. Singh, H. Kong, B. Kim, D. H. Kim, H. E. Jeong, K. Y. Suh, *Tribol. Lett.* **2006**, *21*, 31.
[65] S. Kim, M. Sitti, C. Y. Hui, R. Long, A. Jagota, *Appl. Phys. Lett.* **2007**, *91*, 161905.
[66] M. H. Jin, X. J. Feng, L. Feng, T. L. Sun, J. Zhai, T. J. Li, L. Jiang, *Adv. Mater.* **2005**, *17*, 1977.
[67] T. S. Kustandi, V. D. Samper, D. K. Yi, W. S. Ng, P. Neuzil, W. Sun, *Adv. Funct. Mater.* **2007**, *17*, 2211.
[68] W. Zhao, H. Y. Low, *J. Vac. Sci. Technol.* **2006**, *24*, 255.
[69] D. Santos, M. Spenko, A. Parness, S. Kim, M. Cutkosky, *J. Adhes. Sci. Technol.* **2007**, *21*, 1317.
[70] M. T. Northen, K. L. Turner, *Sens. Actuator, A* **2006**, *130*, 583.
[71] E. Cheung, M. Sitti, *J. Adhes. Sci. Technol.* **2008**, *22*, 569.
[72] A. Peressadko, N. Hosoda, B. N. J. Persson, *Phys. Rev. Lett.* **2005**, *95*, 124301.
[73] E. Verneuil, B. Ladoux, A. Buguin, P. Silberzan, *J. Adhes.* **2007**, *83*, 449.
[74] M. T. Northen, K. L. Turner, *Curr. Appl. Phys.* **2006**, *6*, 379.
[75] T. Thomas, A. J. Crosby, *J. Adhes.* **2006**, *82*, 311.
[76] J. Liu, C.-Y. Hui, L. Shen, A. Jagota, *J. R. Soc. Interface* **2008**, *5*, 1087.
[77] N. J. Glassmaker, A. Jagota, C. Y. Hui, *Acta Biomater.* **2005**, *1*, 367.
[78] N. J. Glassmaker, A. Jagota, C. Y. Hui, W. L. Noderer, M. K. Chaudhury, *Proc. Natl. Acad. Sci. U. S. A.* **2007**, *104*, 10786.
[79] B. X. Zhao, N. Pesika, K. Rosenberg, Y. Tian, H. B. Zeng, P. McGuiggan, K. Autumn, J. Israelachvili, *Langmuir* **2008**, *24*, 1517.
[80] B. X. Zhao, N. Pesika, H. B. Zeng, Z. S. Wei, Y. F. Chen, K. Autumn, K. Turner, J. Israelachvili, *J. Phys. Chem. B* **2009**, *113*, 3615.
[81] H. Zeng, N. Pesika, Y. Tian, B. Zhao, Y. Chen, M. Tirrell, K. L. Turner, J. Israelachvili, *Langmuir* **2009**, *25*, 7486.
[82] C. Majidi, R. E. Groff, Y. Maeno, B. Schubert, S. Baek, B. Bush, R. Maboudian, N. Gravish, M. Wilkinson, K. Autumn, R. S. Fearing, *Phys. Rev. Lett.* **2006**, *97*. 076103.
[83] B. Schubert, C. Majidi, R. E. Groff, S. Baek, B. Bush, R. Maboudian, R. S. Fearing, *J. Adhes. Sci. Technol.* **2007**, *21*, 1297.
[84] J. Lee, R. S. Fearing, K. Komvopoulos, *Appl. Phys. Lett.* **2008**, *93*, 191910.
[85] L. Ge, S. Sethi, L. Ci, P. M. Ajayan, A. Dhinojwala, *Proc. Natl. Acad. Sci. U. S. A.* **2007**, *104*, 10792.
[86] Y. Zhao, T. Tong, L. Delzeit, A. Kashani, M. Meyyappan, A. Majumdar, *J. Vac. Sci. Technol. B* **2006**, *24*, 331.
[87] L. T. Qu, L. M. Dai, M. Stone, Z. H. Xia, Z. L. Wang, *Science* **2008**, *322*, 238.
[88] Y. Maeno, Y. Nakayama, *Appl. Phys. Lett.* **2009**, *94*.
[89] H. Yao, G. D. Rocca, P. R. Guduru, H. Gao, *J. R. Soc. Interface* **2008**, *5*, 723.
[90] Y. Tian, N. Pesika, H. B. Zeng, K. Rosenberg, B. X. Zhao, P. McGuiggan, K. Autumn, J. Israelachvili, *Proc. Natl. Acad. Sci. U. S. A.* **2006**, *103*, 19320.
[91] B. Schubert, J. Lee, C. Majidi, R. S. Fearing, *J. R. Soc. Interface* **2008**, *5*, 845.
[92] M. Lamblet, E. Verneuil, T. Vilmin, A. Buguin, P. Solberzan, L. Léger, *Langmuir* **2007**, *23*, 6966.
[93] A. Ghatak, L. Mahadevan, J. Y. Chung, M. K. Chaudhury, V. Shenoy, *Proc. R. Soc. A* **2004**, *460*, 2725.
[94] A. Majumder, A. Ghatak, A. Sharma, *Science* **2007**, *318*, 258.
[95] E. P. Chan, C. H. Ahn, A. J. Crosby, *J. Adhes.* **2007**, *83*, 473.
[96] K. Autumn, A. Dittmore, D. Santos, M. Spenko, M. Cutkosky, *J. Exp. Biol.* **2006**, 206. 3569.
[97] Y. Tian, N. Pesika, H. Zeng, K. Rosenberg, B. Zhao, P. McGuiggan, K. Autumn, J. N. Israelachvili, *Proc. Natl. Acad. Sci. U. S. A.* **2006**, *103*, 19320.
[98] B. Aksak, M. Sitti, A. Cassell, J. Li, M. Meyyappan, P. Callen, *Appl. Phys. Lett.* **2007**, *91*.
[99] D. S. Kim, H. S. Lee, J. Lee, S. Kim, K. H. Lee, W. Moon, T. H. Kwon, *Microsyst. Technol.* **2007**, *13*, 601.
[100] S. Kim, B. Aksak, M. Sitti, *Appl. Phys. Lett.* **2007**, *91*.
[101] M. Schargott, V. K. Popov, S. Gorb, *J. Theor. Biol.* **2006**, *243*, 48.
[102] M. Schargott, *Bioinspir. Biomim.* **2009**, 026002.
[103] R. Long, C. Y. Hui, *Proc. R. Soc. A* **2009**, *465*, 961.
[104] J. Y. Chung, M. K. Chaudhury, *J. R. Soc. Interface* **2005**, *2*, 55.
[105] M. T. Northen, C. Greiner, E. Arzt, K. L. Turner, *Adv. Mater.* **2008**, *20*, 3905.
[106] E. Kroner, E. J. De Souza, M. Kamperman, E. Arzt, unpublished results **2009**.
[107] M. Varenberg, A. Peressadko, S. Gorb, E. Arzt, S. Mrotzek, *Rev. Sci. Instrum.* **2006**, *77*.
[108] M. Varenberg, S. Gorb, *J. R. Soc. Interface* **2007**, *4*, 721.

[109] E. J. De Souza, M. Kamperman, G. Castellanos, R. M. McMeeking, E. Arzt, to be published **2010**.
[110] A. del Campo, I. Álvarez, S. Filipe, M. Wilhelm, *Adv. Funct. Mater.* **2007**, *17*, 3590.
[111] K. Seok, B. Aksak, M. Sitti, *Appl. Phys. Lett.* **2007**, *22*, 1913.
[112] H. Yao, H. Gao, *J. Mech. Phys. Solids* **2006**, *54*, 1120.
[113] H. Yao, G. Della Rocca, P. R. Guduru, H. Gao, *J. R. Soc. Interface* **2008**, *5*, 723.
[114] B. Bhushan, A. Peressadko, T. W. Kim, *J. Adhes. Sci. Technol.* **2006**, *20*, 1475.
[115] T. W. Kim, B. Bhushan, *Ultramicroscopy* **2007**, *107*, 902.
[116] P. K. Porwal, C. Y. Hui, *J. R. Soc. Interface* **2008**, *5*, 441.
[117] C. Greiner, E. Arzt, A. del Campo, *Adv. Mater.* **2009**, *21*, 479.
[118] M. P. Murphy, S. Kim, M. Sitti, *ACS Appl. Mater. Interfaces* **2009**, *1*, 849.
[119] C. Greiner, S. Buhl, A. del Campo, E. Arzt, *J. Adhes.* **2009**, *85*, 646.
[120] R. Long, C. Y. Hui, S. Kim, M. Sitti, *J. Appl. Phys.* **2008**, *104*.
[121] G. Guidoni, D. Schillo, U. Hangen, G. Castellanos, E. Arzt, R. M. McMeeking, R. Bennewitz, to be published **2010**. Submitted.
[122] S. Buhl, C. Greiner, A. del Campo, E. Arzt, *Int. J. Mater. Res.* **2009**, *100*, 1119.
[123] D. Dodou, A. Del Campo, E. Arzt, *2007 Annual Intern. Conf. IEEE Eng. in Medicine and Biology Society (EMBC '07)*, IEEE Service Center, Piscataway, NJ **2007**, p. 1457.
[124] A. Mahdavi, L. Ferreira, C. Sundback, J. W. Nichol, E. P. Chan, D. J. D. Carter, C. J. Bettinger, S. Patanavanich, L. Chignozha, E. Ben-Joseph, A. Galakatos, H. Pryor, I. Pomerantseva, P. T. Masiakos, W. Faquin, A. Zumbuehl, S. Hong, J. Borenstein, J. Vacanti, R. Langer, J. M. Karp, *Proc. Natl. Acad. Sci. U. S. A.* **2008**, *105*, 2307.
[125] E. J. De Souza, M. Kamperman, G. Castellanos, E. Kroner, V. Armbrüster, M. S. Romann, B. Schick, E. Arzt, *31st Annual International IEEE EMBS Conference* **2009**. Minneapolis, September 2–6, 2009.
[126] S. Reddy, E. Arzt, A. Del Campo, *Adv. Mater.* **2007**, *19*, 3833.
[127] K. Autumn, *Am. Sci.* **2006**, *94*, 124.
[128] L. Qu, L. Dai, *Adv. Mater.* **2007**, *19*, 3844.
[129] T. W. Kim, B. Bhushan, *J. Vac. Sci. Technol, A* **2007**, *25*, 1003.
[130] W. K. Cho, I. S. Choi, *Adv. Funct. Mater.* **2008**, *18*, 1089.
[131] J. Lee, R. S. Fearing, *Langmuir* **2008**, *24*, 10587.
[132] G. W. Lu, W. J. Hong, L. Tong, H. Bai, Y. Wei, G. Q. Shi, *ACS Nano* **2008**, *2*, 2342.
[133] J. Lee, C. Majidi, B. Schubert, R. S. Fearing, *J. R. Soc. Interface* **2008**, *5*, 835.
[134] J. Lee, B. Bush, R. Maboudian, R. S. Fearing, *Langmuir* **2009**, *25*, 12449.
[135] N. J. Glassmaker, C. Y. Hui, *J. Appl. Phys.* **2004**, *96*, 3429.
[136] H. Lee, B. P. Lee, P. B. Messersmith, *Nature* **2007**, *448*, 338.
[137] P. Glass, H. Chung, N. R. Washburn, M. Sitti, *Langmuir* **2009**, *25*, 6607.
[138] T.-I. Kim, H. E. Jeong, K. Y. Suh, H. H. Lee, *Adv. Mater.* **2009**, *21*, 2276.
[139] H. Yoon, H.-E. Jeong, T. Kim, T. J. Kang, D. Tahk, K. Char, K. Y. Suh, *Nano Today* **2009**, *42*, 385.

